An LIF characterization of supersonic BO (X2+) and CN (X2+) radical sources for crossed beam studies

Pavlo Maksyutenko, Dorian S. N. Parker, Fangtong Zhang and Ralf I. Kaiser

Related Articles

New method for the calibration of three-dimensional atom-probe mass spectra
Rev. Sci. Instrum. 72, 2984 (2001)

Energy distribution and spatial structure of electrosprays of ionic liquids in vacuo
J. Appl. Phys. 95, 2123 (2004)

Recent results with Au ions from a multiampere electron beam ion source at Brookhaven National Laboratory (invited abstract)
Rev. Sci. Instrum. 75, 1542 (2004)

Time-of-flight secondary ion mass spectroscopy for surface analysis of insulators using a cluster ion beam
Appl. Phys. Lett. 83, 4872 (2003)

Quantitative analysis of transient surface reactions on planar catalyst with time-resolved time-of-flight mass spectrometry
Rev. Sci. Instrum. 78, 104102 (2007)

Additional information on *Review of Scientific Instruments*

Journal Homepage: rsi.aip.org

Journal Information: rsi.aip.org/about/about_the_journal

Top downloads: rsi.aip.org/features/most_downloaded

Information for Authors: rsi.aip.org/authors

An LIF characterization of supersonic BO (X²Σ⁺) and CN (X²Σ⁺) radical sources for crossed beam studies

Pavlo Maksyutenko, Dorian S. N. Parker, Fangtong Zhang, and Ralf I. Kaiser
Department of Chemistry, University of Hawaii at Manoa, Honolulu, Hawaii 96822, USA

Various ablation sources generating supersonic boron monoxide (BO; $X^2\Sigma^+$) radical beams utilizing oxygen (O_2), carbon dioxide (CO_2), methanol (CH_3OH), and water (H_2O) as seeding gases were characterized in a crossed molecular beams setup by mass resolved time-of-flight spectroscopy and spectroscopically via laser induced fluorescence. Intensities of the sources as well as rovibrational energy distributions were analyzed. The molecular oxygen source was found to produce excessive amount of an unwanted BO_2 byproduct. Internal vibrational energy of boron monoxide generated in the water and methanol sources was too high to be considered for the study of dynamics of ground state radicals. The best combination of intensity, purity, and low internal energy was found in the carbon dioxide source to generate boron monoxide. We successfully tested the boron monoxide (BO; $X^2\Sigma^+$) radical beam source in crossed beams reactions with acetylene (C_2H_2) and ethylene (C_2H_4). The source was also compared with supersonic beams of the isoelectronic cyano (CN; $X^2\Sigma^+$) radical. © *2011 American Institute of Physics*. [doi:10.1063/1.3624695]

I. INTRODUCTION

Conventional air-breathing rocket propulsion systems rely on oxidation of hydrocarbons. Tight gravimetric and volumetric energy capacity requirements led to the research on alternative fuels. Boron is a promising candidate as a dopant for hydrocarbon fuels. The energy of complete oxidation of boron to diborontrioxide (B_2O_3) is three times greater than that of most hydrocarbon jet fuels. The oxidation of boron occurs via the schematic reaction sequence $B \rightarrow BO \rightarrow BO_2 \rightarrow B_2O_3$.[1] The formation of boron monoxide (BO; $X^2\Sigma^+$) is the very first oxidation step. Taking into account its stability under combustion conditions, the reactions of boron monoxide with combustion species such as hydrocarbons deserve considerable attention. Although the reaction dynamics of boron atoms with hydrocarbon molecules[2] such as acetylene (C_2H_2),[3–5] ethylene (C_2H_4),[6,7] benzene (C_6H_6),[8,9] allene (C_3H_2),[10] dimethylacetylene ($CH_3C_2CH_3$),[11] and methylacetylene (CH_3C_2H) (Ref. [12]) were unraveled utilizing the crossed molecular beam approach, the reaction dynamics of boron monoxide (BO; $X^2\Sigma^+$) with hydrocarbons have neither been investigated experimentally nor theoretically to date. However, the elucidation of the chemical dynamics of this reaction class is crucial to develop reliable models of boron combustion systems.

In order to initiate a systematic dynamics research of these reactions utilizing a crossed beam setup, we develop here an ablation source of boron monoxide radicals relying on reaction of ablated boron atoms with oxygen-bearing molecules undergoing supersonic expansion. The four gases of choice were molecular oxygen, carbon dioxide, methanol, and water. Rate constants of boron reactions with these reactants were measured previously by Davidovits *et al.*[13,14] at room temperature. The integral rate constants were found to be $4.6 \pm 1.8 \times 10^{-11}$, $7.0 \pm 2.8 \times 10^{-14}$, $1.3 \pm 0.5 \times 10^{-10}$, and $4.7 \pm 1.9 \times 10^{-12}$ for oxygen, carbon dioxide, methanol,

and water, respectively. The reaction with oxygen has no entrance barrier[15] while 80 and 21 kJ mol⁻¹ barriers[16,17] need to be overcome in interaction with carbon dioxide and water. To our best knowledge there was no study of boron monoxide formation in interaction with methanol. In this paper, we characterize the intensity of boron monoxide and the efficiency of supersonic rovibrational cooling of these radicals in a supersonic beam by combined mass-selected time-of-flight (TOF) and laser induced fluorescence (LIF) studies. Since there are no previous LIF studies of boron monoxide supersonic beams to compare with our results, we also characterized in the same experimental geometry the supersonic beam of cyano radicals (CN; $X^2\Sigma^+$), which are isoelectronic to boron monoxide (BO; $X^2\Sigma^+$). This helps to understand the supersonic cooling and hence basic collisional energy transfer processes to cool isoenergetic radicals in distinct carrier gases.

II. EXPERIMENTAL SETUP

The characterization of supersonic beams of boron monoxide and cyano radicals was carried out in a crossed molecular beams machine at the University of Hawaii.[13] A supersonic beam of ground state boron monoxide, BO ($X^2\Sigma^+$), was produced by reaction of ablated boron atoms in pulsed supersonic flows of different oxygen-containing neat gases or gas mixtures. The four options tested in the present study are molecular oxygen (99.9999%, BOC gases), carbon dioxide (99.9999%, BOC gases); water, and methanol vapor were produced by bubbling helium carrier gas (99.9999% Airgas) through a stainless steel containers with liquid samples at room temperature (293 K). The optimized pressures and molar fractions for water and methanol are summarized in Table I. Boron was ablated by focusing 3 to 10 mJ output of the 4th harmonic (266 nm) of a Spectra-Physics Quanta-Ray Pro 270 Nd:YAG laser operating at 30 Hz onto a boron rod performing helical motion. The isotopically natural boron

82, 083107-1

TABLE I. Experimental conditions, characterization by QMS-TOF (peak velocity and integrated intensity of BO and BO_2) and by LIF (rotational-vibrational state distribution) for the different sources of boron monoxide.

Gas	Ablation laser power (mJ)	$D_1/D_2/D_3$,[a] (μs)	Speed ratio, v_p, ms^{-1}	Integrated QMS-TOF (a.u.)		Rotational-vibrational state distribution from LIF spectra	
				BO	BO_2	v = 0	v = 1
O_2 4 bars	10	1844/ 16 670/ 37	1215 3.3	1	1.17	90% T_{rot} = 350 K	<10%
CO_2 4 bars	9	1840/ 16 670/ 48	1010 4.6	0.78	N/A	95% T_{rot} = 250 K	<5%
CH_3OH 2.8% in 6 bars He	3.5	1871/ 16 655/ 20	1905 4.0	0.74	0.17	90% T_{rot} = 140 K	10% T_{rot} = 100 K
H_2O 0.5% in 6 bars He	3.5	1871/ 16 653/ 18	1880 5.4	0.65	0.03	90% T_{rot} = 120 K	10% T_{rot} = 100 K

[a]Electronic delays in Figure 2.

rod (80% ^{11}B, 20% ^{10}B) was mounted on a homemade ablation source[14] placed in the primary source region of the vacuum chamber. The seeding gas was introduced via a Proch-Trickl piezo-electric pulsed valve, operating at 60 Hz repetition rate. The molecular beam containing boron monoxide passed a skimmer and a four-slit chopper wheel, which selected a segment of the beam of a well-defined peak velocity and speed ratio. The beam characteristics are compiled in Table I. To characterize isoelectronic radical beams and investigate the dependence on the rotational and vibrational temperatures, a supersonic beam of ground state cyano radicals, CN($X^2\Sigma^+$), was produced by reaction of ablated carbon atoms with pulsed supersonic flow of nitrogen gas (99.9999%, Airgas).[15] The carbon was ablated by 12 mJ pulses of focused 266 nm laser radiat1ion. The beam characteristics are summarized in Table II.

We characterized the rovibrational energy distribution within the ground electronic states of boron monoxide and cyano radicals employing LIF. The geometry of the LIF detection is shown in Fig. 1 with the pulse sequence compiled in Fig. 2. The main experimental challenge of the LIF measurement was to suppress the scattered laser light in a tight volume of the crossed beams setup. To achieve this, the detection laser beam was focused to a 2 mm diameter spot at the crossing point by a 1.5 m lens. A baffle tube containing eight irises of 4 mm and 5 mm diameter trapped divergent components in the detection laser beam. The incoming detection laser beam was mainly absorbed by a piece of polished black glass (ThorLabs; neutral density filter OD6; 40–20 surface quality); the reflected part traveled back into the baffle tube. A spatial filtering of fluorescence light was introduced. The fluorescence spot in the interaction region was projected

TABLE II. Experimental conditions (electronic delays), characterization by QMS-TOF (peak velocity) and by LIF (rotational-vibrational state distribution) for the different velocities of cyano radical beam.

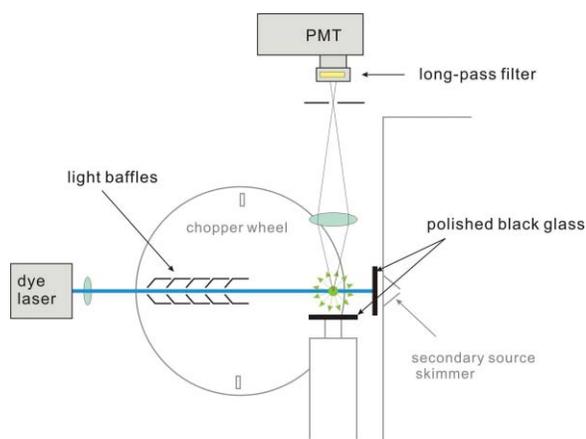| Speed ratio, v_p, m s^{-1}	$D_1/D_2/D_3$,[a] (μs)	Rotational-vibrational state distribution				
		v = 0 Fraction (%)	T_{rot} (K)	v = 1 Fraction (%)	T_{rot} (K)	v = 2 Fraction (%)
1880 2.2	1853/ 16 679/ 44	42 26	1500 400	13 8	1500 400	11
1720 2.4	1850/ 16 679/ 50	46 19	1500 400	14 7	1500 400	14
1550 2.6	1845/ 16 680/ 49	51 23	1500 300	10 7	1500 300	9
1400 3.1	1840/ 16 680/ 60	47 29	1500 300	9 6	1500 300	9
1240 4.1	1832/ 16 681/ 73	47 29	1300 160	9 6	1300 160	9
1065 5.2	1824/ 16 682/ 73	48 43	1300 120	9	300	<5

[a]Electronic delays in Figure 1.

FIG. 1. (Color online) Schematic geometry of the laser induced fluorescence detection setup as incorporated in the crossed beams machine.

by a 35 mm focus lens onto the center of the iris in front of the photomultiplier tube (PMT), which had been mounted on the lid of the machine. This vertical orientation of the detector also allowed us to minimize the collection of Raleigh scattered light of the vertically polarized laser on the atoms and molecules in the beam. Another piece of polished black glass was placed under the interaction region to eliminate the propagation of scattered laser light in the light collection cone.

The electronic ground state of the boron monoxide radical was probed via $A^2\Pi_i$–$X^2\Sigma^+$ (0, 0) and (1, 1) vibrational bands at ∼425 and ∼434.5 nm by the pulsed 10 μJ output of a Lambda Physik Scanmate dye laser pumped by the third harmonic of an integrated Nd:YAG laser operating at 10 Hz with an output power of 50 mJ per pulse. The dye laser was delayed relative to the pulse valve opening time to intercept the peak of the boron monoxide beam. The timing of the experiment is

presented in detail in Figure 1. The fluorescence was detected by a Hamamatsu R955 PMT filtered by a Schott color glass long-pass GG-495 filter for, e.g., (2, 0) and (3, 1), fluorescence detection and scattered detection laser light suppression. The signal was then amplified by a built-in amplifier of the Hamamatsu C7247 PMT socket assembly and filtered by a high pass filter prior to feeding into a digital oscilloscope interfaced to a computer for data collecting and processing. The LIF spectra were then analyzed utilizing diatomic spectral simulation program by Tan.[16] We adopted spectroscopic constants for the $A^2\Pi_i$–$X^2\Sigma^+$ system from Melen *et al.*[17] and Franck-Condon factors from Liszt *et al.*[18] The electronic ground state of the cyano radical was probed via $B^2\Sigma^+$–$X^2\Sigma^+$ (0, 0), (1, 1), and (2, 2) vibrational bands at ∼387 nm by the pulsed 4 μJ output of a Lambda Physik Scanmate dye laser. No optical filters were mounted in front of the PMT.

As compiled in Fig. 2, the 17 cm diameter four-slit chopper wheel with 0.76 mm slits operated at 120 Hz between the skimmer of the primary source and the interaction region. An infrared diode attached to the top of the chopper unit provided the time zero of the experiment by detecting the slit passage. The time delay between the diode pulse and the pulsed valve determined a distinct part of the molecular beam that could pass through the chopper slit. An SRS DG535 delay/pulse generator (PDG I) was triggered at 60 Hz by the frequency divided output of the diode. The output of the pulse generator (50 Ω, +3.5 V, 80 μs pulse width) leads to a homemade pulse shaper, which in turn was connected to the Physik Instumente P-286.23 high voltage pulse amplifier. The output of the amplifier drove a piezoelectric Proch–Trickl valve at repetition rate of 60 Hz, −400 V amplitude and 80 μs duration. A second output of the PDG I pulse generator (TTL, high impedance) passed a frequency divider (division by two,
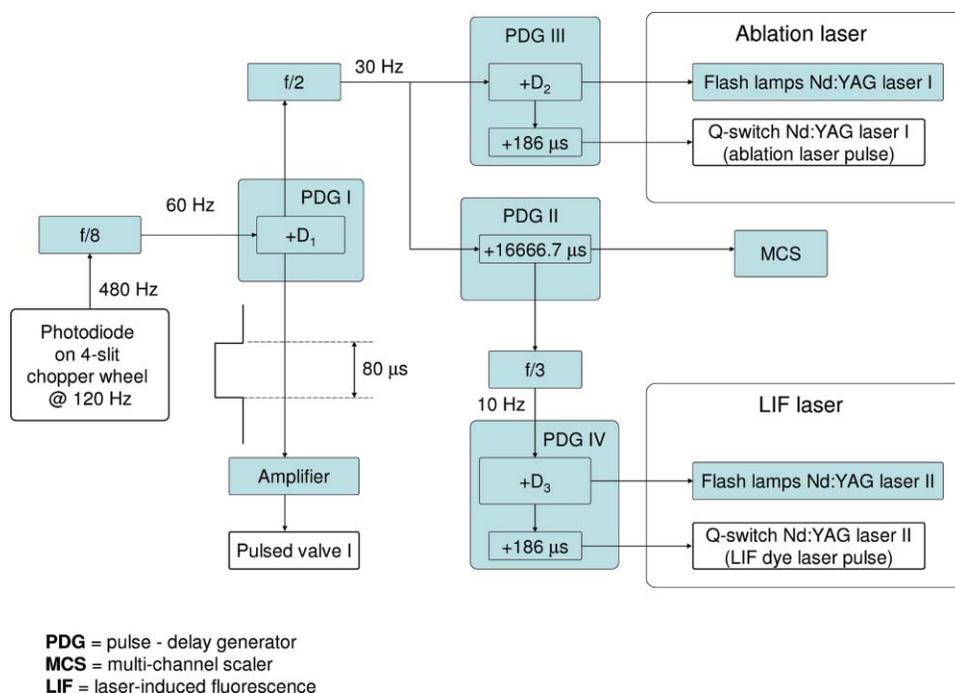

PDG = pulse - delay generator
MCS = multi-channel scaler
LIF = laser-induced fluorescence

FIG. 2. (Color online) Pulse sequence for the crossed beams experiments and LIF detection. Delay times D_1, D_2, and D_3 differ for distinct boron monoxide or cyano beams produced in the primary chamber. These delays are summarized in Tables I and II for boron monoxide and cyano, respectively.

50 Ω output) and acted as an external trigger to a second delay/pulse generator (PDG II). Its time delayed output (T_0 +16 666.66 μs, high impedance TTL) was fed into the SRS 430 multichannel scaler (MCS) utilizing trigger and discriminator levels of +0.5 and +0.2 V. A third output of the frequency divider served as an external trigger of PDG III. This unit controls the time sequence of Spectra Physics Nd:YAG laser. Channel AB (A = T_0 + D_2, B = A + 5 μs, 50 Ω, TTL) triggered the flash lamps and CD the Q-switch (C = A + 186 μs, D = C + 5 μs, 50 Ω, TTL). The time sequence for Nd:YAG pumped dye laser (10 Hz repetition rate) used for LIF detection was set by PDG IV triggered by the frequency divided A output of PDG II. Channel AB (A = T_0 + D_3, B = A + 5 μs, 50 Ω, TTL) triggered the flash lamps and CD the Q-switch (C = A + 186 μs, D = C + 5 μs, 50 Ω, TTL) of the internal Nd:YAG laser. Delays for the primary pulsed valve and ablation laser (D_1 and D_2) were optimized to the highest intensity of the radical beam with desired velocity. LIF detection laser delay (D_3) was adjusted to intercept the peak of the radical beam. Delays D_1–D_3 are listed in Tables I and II.

III. RESULTS

Both boron monoxide and cyano radicals are expected to be exclusively in their ground electronic state, $X^2\Sigma^+$, by the time they reach the interaction region of the crossed beams machine. The radiative lifetimes of the first excited electronic state, $A^2\Pi_{\pm1/2}$, of boron monoxide[19] or cyano radicals[20] are short (~1.8 and ~11 μs, respectively) compared to the flight time of few 10 μs from the ablation region to the intersection point. For this reason our LIF study is aimed at probing the rovibrational states on the ground electronic potential surface.

A. BO radical sources

Four oxygen-bearing molecules were tested for the reaction with ablated boron atoms to form boron monoxide: oxygen, carbon dioxide, methanol, and water vapor in helium buffer gas. Four parameters have been varied to maximize the number of produced radicals. These are the ablation laser power, backing pressure in the pulsed valve, and two delay times between the pulsed valve opening and the chopper wheel slit passing the skimmer and between pulsed valve opening and ablation laser pulse. The optimized beams were characterized by on-axis time-of-flight spectra of quadruple mass spectrometer selected species (QMS-TOF) and LIF simultaneously. The mass selected TOF at m/z = 27 provides information on the intensity of ^{11}BO, peak velocity, speed ratio of the beam. Excitation LIF spectra utilizing $A^2\Pi_i$–$X^2\Sigma^+$ transitions in (0, 0) and (1, 1) vibrational bands allow us to probe the populated rovibrational states. The LIF spectra for different seeding gasses are compiled in Fig. 3, and characteristics derived from these spectra and QMS-TOF spectra are included in Table I.

1. B + O₂

Integral counts for ^{11}BO (m/z = 27) derived from integrated TOF spectrum are the highest among all measured BO
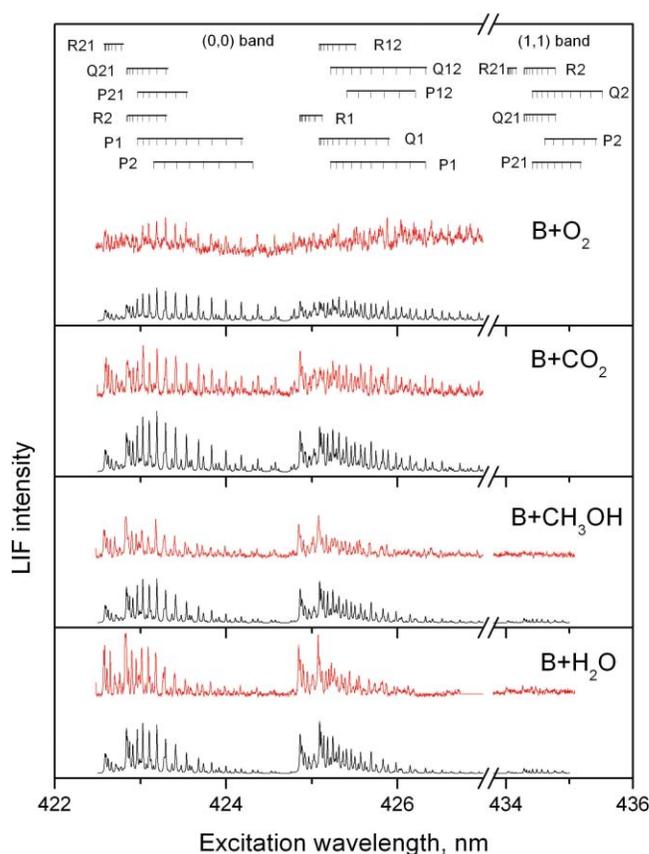

FIG. 3. (Color online) LIF excitation spectra of $A^2\Pi_i$–$X^2\Sigma^+$ system in (0, 0) and (1, 1) vibrational bands of boron monoxide. Experimental spectra (upper curves) and best-fit simulations (lower curves) are shown for different boron oxide sources. The double headed appearance of the spectrum is caused by spin-orbit splitting of the upper state. Rotational assignment is shown for ^{11}BO (0, 0) band. Intensity scale is kept the same to represent relative intensities of different sources.

sources. However, ^{11}BO$_2$ (m/z = 43) is formed in this source with comparable intensity. The best fit of LIF spectrum in (0, 0) vibrational band assumes 350 K rotational temperature. The rotational cooling is the worst among the sources (T_{rot} = 350 K). Poor translational cooling is reflected in the low speed ratio (S = 3.3) of the beam. The peak velocity, 1215 ms^{-1}, is defined mostly by oxygen seeding gas supersonic beam velocity. The BO spectrum is superimposed with the background fluorescence of BO$_2$ of comparable intensity supporting QMS-TOF observation of this species. We did not observe any transitions in (1, 1) band (~435 nm). Based on the relatively high background noise we estimate that less than 10% BO radicals populate v = 1 vibrational level in the beam.

2. B + CO₂

Integral counts for ^{11}BO are about 20% lower for the CO$_2$ seeding gas. Signal of BO$_2$ could not be measured because of the interferences from CO$_2$ ion signal. Although, the apparent absence of broad feature in LIF spectrum arising from BO$_2$ fluorescence suggests smaller probability of BO$_2$ formation in CO$_2$ than in O$_2$. The rotational temperature is 250 K. Speed ratio is 4.6, peak velocity is 1010 ms^{-1}. The double headed appearance of the spectrum caused by spin-orbit splitting of

the upper electronic state is evident at this lower temperature. We did not observe any transitions in the (1, 1) band either. Accounting for the lower background noise we estimate that less than 5% BO radicals populate v = 1 vibrational levels in the supersonic beam.

3. B + CH₃OH

Integral counts for ^{11}BO are close to those for CO_2 seeding gas. BO_2 relative to BO production is 5 times smaller than in O_2. The rotational temperature in v = 0 is 140 K revealing a good cooling capacity of helium buffer gas. The speed ratio was measured to be 4.0, whereas the peak velocity was determined to be 1905 ms^{-1}. The vibrationally excited fraction (v = 1) is ~10% with rotational temperature ~100 K.

4. B + H₂O

The integral counts for ^{11}BO are 15% lower than in the case of CO_2 seeding gas. BO_2 relative to BO production is 30 times smaller than in O_2. The rotational temperature in v = 0 is 120 K, the lowest among all studied sources. Correspondingly, the speed ratio is the highest, S = 5.4. The peak velocity of BO radicals entrained in helium supersonic beam is 1880 ms^{-1}. Vibrationally excited (v = 1) fraction is ~10% with rotational temperature ~100 K.

5. Crossed beams reaction with acetylene and ethylene

We verified the feasibility of the boron monoxide source generated via laser ablation of boron atoms seeded in carbon dioxide carrier gas in crossed beams reactions with acetylene (C_2H_2; $X^1\Sigma_g^+$) and ethylene (C_2H_4; X^1A_g). Supersonic beam of boron monoxide crossed perpendicularly the segments of supersonic acetylene and ethylene beams with peak velocities $v_p = 900 \pm 10$ and 890 ± 10 ms^{-1} and with the speed ratios of 9.0 ± 0.2 and 7.0 ± 0.2 correspondingly. The QMS-TOF scans of the heavy products of the atomic hydrogen loss channel close to the center-of-mass angles are shown in Fig. 4. Op-
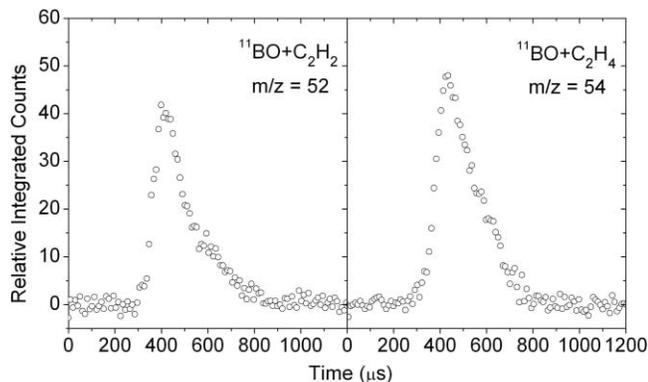

FIG. 4. Time-of-flight spectra for the crossed beams reactions of boron monoxide (^{11}BO; $X^2\Sigma^+$) with acetylene (C_2H_2; $X^1\Sigma_g^+$) at a collision energy of 13.0 ± 0.8 kJ mol^{-1} (left) and with ethylene (C_2H_4; X^1A_g) at a collision energy of 12.4 ± 0.6 kJ mol^{-1}(right). Heavy products of the atomic hydrogen loss channels at m/z = 52 and 54 are selected. 2.6×10^5 TOF spectra are averaged.
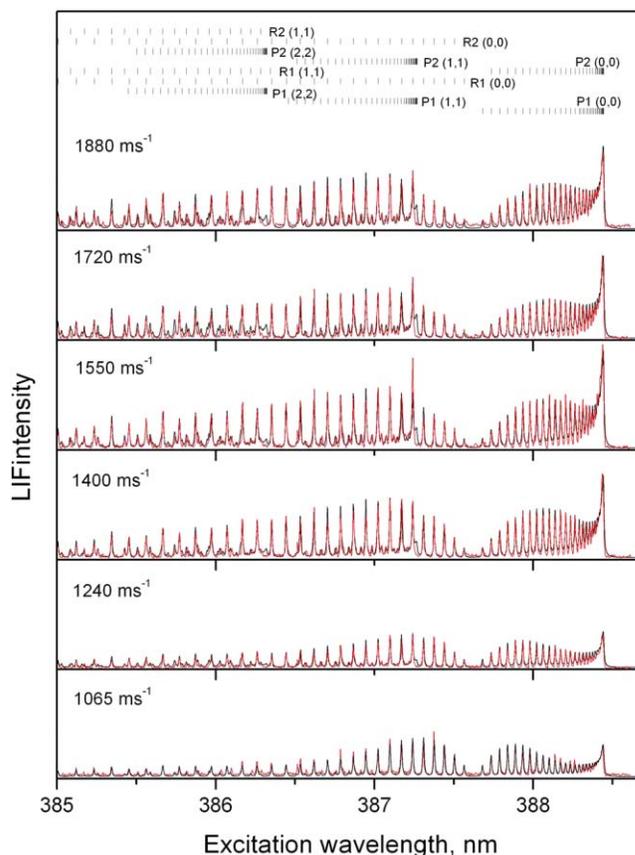

FIG. 5. (Color) LIF excitation spectra of $B^2\Sigma^+$–$X^2\Sigma^+$ system in (0, 0), (1, 1), and (2, 2) vibrational bands of cyano radicals. Experimental spectra (red curves) and best-fit simulations (black curves) are shown for the specified peak velocities of cyano radical beam. Intensity scale is kept the same to represent relative intensities of the beams with different velocities.

eration of secondary pulsed valve at 60 Hz enabled laser-on / laser-off subtraction. The detection angle was set close to the center-of-mass angles of $38.3° \pm 1.2°$ and $41.1° \pm 1.0°$ for $^{11}BO + C_2H_2$ and $^{11}BO + C_2H_4$ systems correspondingly. Averaging of 2.6×10^5 TOF spectra (~2.5 h scan at 30 Hz repetition rate) produces a good signal-to-noise.

B. CN radical source

Variation of the pulsed valve delay relative to the chopper wheel trigger pulse and ablation laser delay relative to pulsed valve allowed us to select the peak velocities of cyano beam in the range from 1065 to 1880 ms^{-1}. We characterized the optimized beams at different peak velocities in this range in 150 ms^{-1} step. The LIF spectra for different velocities are compiled in Fig. 5, and characteristics derived from these spectra and QMS-TOF spectra are included in Table II. The rotational population distribution was found to be nonthermal. The LIF spectra cannot be simulated with a single rotational temperature, while with two temperatures simulations produce good fits. We will address this observation in Sec. IV C.

IV. DISCUSSION

A. Comparison of BO sources

Depending on the second reactant and other details of a crossed beam study the choice of a boron monoxide source may vary. Below we will list the advantages and disadvantages of the different sources. The boron monoxide production is the highest in reaction with O_2 seeding gas, but this source should be avoided if BO_2 reactant is undesirable. Also, the supersonic cooling in O_2 is the poorest as represented by rotational temperature (350 K) and speed ratio (S = 3.3). Although the interference from BO_2 in the LIF spectrum precludes accurate detection of vibrationally excited BO, vibrational relaxation in collisions with O_2 is expected to be slow because of significant mismatch in vibrational frequency with BO (Ref. [21]) (1862 cm^{-1} fundamental frequency for BO versus 1556 cm^{-1} for O_2). Considering these shortcomings, the CO_2 source might be preferred for low velocity BO. The rotational temperature is lower (250 K), and higher speed ratio (S = 4.6) indicates better cooling. Vibrational cooling is expected to be faster due to strong coupling of ^{11}BO vibration (1862 cm^{-1} fundamental) to $\nu_1 + \nu_2$ vibration (1955 cm^{-1}) in CO_2. The two higher velocity options, methanol and water vapor in helium buffer gas, give similar results in terms of BO production efficiency (10% higher for methanol) and rotational temperature (15% lower for water). The biggest difference is in BO_2 byproduct. Water source is 7 times cleaner, while methanol source is still 5 times cleaner than oxygen source. The supersonic cooling in helium buffer gas is rather efficient, especially for rotational degrees of freedom, because higher velocity light atoms provide more collisions per time unit. About 10% of BO radicals are in the first vibrationally excited state. Therefore, in order to only probe the reaction dynamics of ground state boron monoxide, these two sources should be avoided.

Based on these observations we would recommend utilizing a supersonic boron monoxide beam obtained from carbon dioxide seeding gas for reaction dynamics studies. Test crossed beams reactions with acetylene and ethylene directly demonstrate its applicability to conduct crossed molecular beam reactions with unsaturated hydrocarbon molecules.

B. Comparison of BO and CN sources

Apart from differences in rotational population due to bimodal distribution in the cyano radical as discussed in Sec. III B, we also observe higher population of vibrationally excited states in CN than in BO. Several causes can be considered. First, the temperature of the plasma formed in ablation process is likely to be higher for graphite since its absorption peak, ~260 nm,[22] is very close to the ablation laser wavelength, 266 nm. Second, in the reaction of carbon atom with nitrogen only cyano product can carry internal excitation, whereas in boron reactions with methanol, carbon dioxide or water di- or polyatomic co-products can take significant fraction of vibrational excitation. Third, the cooling efficiencies of CN and BO radicals in supersonic expansion are different. Vibrational relaxation[21] of the cyano radical vibrations

(2042 cm^{-1} fundamental frequency) in molecular nitrogen (2330 cm^{-1}) is non-resonant due to the large energy difference in vibrational quanta. The vibrational quenching here is governed by a weaker vibrational-translational coupling and may be not completed during collisional phase of supersonic expansion. Vibrations in ^{11}BO (1862 cm^{-1} fundamental frequency) can be coupled more efficiently to those in CO_2 ($\nu_1 + \nu_2 = 1955$ cm^{-1}). In the case of helium buffer gas the non-resonant vibrational relaxation is efficient due to a high collision rate.

C. Internal energy distribution of CN beam

Analysis of the LIF spectra of cyano radicals in supersonic beams traveling at different velocities (Table II) reveals a bimodal rotational energy distribution. This fact is in agreement with observation by Hay *et al.*[23] that highly rotationally excited cyano radicals (n > 60) are essentially collisionally metastable surviving hundreds of collisions with the nitrogen buffer gas following 193 nm BrCN photolysis. This behavior has been confirmed by the study of photolytic cyano radical reactions in Ar buffer gas.[24,25] The recent characterization of continuous supersonic beam of cyano radicals produced in radio-frequency discharge[26] also reveals bimodal rotational distribution with peaks at 250 and 5000 K. The vibrational population in that study was found to be thermal corresponding to 6500 K. The vibrational distribution for our ablation source is much cooler ranging from 1200 K for the slowest beam (1065 ms^{-1}) to 3000 K for the fastest one (1880 ms^{-1}). Table II represents vibrational distribution explicitly as population fractions for v = 0, 1, and 2. Bimodal rotational distributions for v = 0 and 1 were found to be essentially identical, whereas a poor signal-to-noise ratio of v = 2 features did not allow adequate determination of rotational distribution. Lower vibrational excitation for ablation source compared to discharge source could be attributable to difference in initial excitation and higher backing pressure in the pulsed valve (translating into better cooling in supersonic expansion) that could be attained in the case of pulsed valves utilized in the ablation source.

V. CONCLUSIONS

Based on boron monoxide radical source intensity, purity (low BO_2 production) and supersonic cooling efficiency, the carbon dioxide source is the most adequate for reaction dynamics studies among the four studied boron ablation sources. The oxygen source produces excessive amount of BO_2; and we discard water and methanol sources based on high (~10%) population of v = 1 vibrationally excited state, which has different energy balance in crossed beam studies and might exhibit a different reaction dynamics. However, further experimental efforts might improve the vibrational cooling efficiency to some extent by adding different collision partners to a carrier gas. We also verified the utility of boron monoxide source based on ablated boron interaction with carbon dioxide beam by recording the center-of-mass TOF spectra of the heavy products in

hydrogen atom loss reactions with acetylene and ethylene in crossed beams. Good signal-to-noise was achieved within reasonable accumulation times demonstrating the potential for the experimental study of reaction dynamics of boron monoxide with hydrocarbons. Finally, compared to a single available previous study of an isoelectronic cyano radical beam produced by a continuous RF discharge source,[26] our pulsed ablation source produces internally colder radicals at similar beam velocity. This can be attributed to better cooling efficiency at higher backing pressure and/or differences in initial excitation in RF discharge and ablation source.

[1] S. H. Bauer, Chem. Rev. **96**(6), 1907 (1996).

[2] N. Balucani, F. Zhang, and R. I. Kaiser, Chem. Rev. **110**(9), 5107 (2010).

[3] F. Zhang, X. Gu, R. I. Kaiser, and H. Bettinger, Chem. Phys. Lett. **450**(4–6), 178 (2007).

[4] L. Andrews, P. Hassanzadeh, J. M. L. Martin, and P. R. Taylor, J. Phys. Chem. **97**(22), 5839 (1993).

[5] R. I. Kaiser, N. Balucani, N. Galland, F. Caralp, M. T. Rayez, and Y. Hannachi, Phys. Chem. Chem. Phys. **6**(9), 2205 (2004).

[6] N. Balucani, O. Asvany, Y. T. Lee, R. I. Kaiser, N. Galland, and Y. Hannachi, J. Am. Chem. Soc. **122**(45), 11234 (2000).

[7] F. Zhang, X. Gu, R. I. Kaiser, N. Balucani, C. H. Huang, C. H. Kao, and A. H. H. Chang, J. Phys. Chem. A **112**(17), 3837 (2008).

[8] F. Zhang, Y. Guo, X. Gu, and R. I. Kaiser, Chem. Phys. Lett. **440**(1–3), 56 (2007).

[9] H. F. Bettinger and R. I. Kaiser, J. Phys. Chem. A **108**(21), 4576 (2004).

[10] F. Zhang, H. L. Sun, A. H. H. Chang, X. Gu, and R. I. Kaiser, J. Phys. Chem. A **111**(51), 13305 (2007).

[11] D. Sillars, R. I. Kaiser, N. Galland, and Y. Hannachi, J. Phys. Chem. A **107**(26), 5149 (2003).

[12] F. Zhang, C. H. Kao, A. H. H. Chang, X. Gu, Y. Guo, and R. I. Kaiser, ChemPhysChem **9**(1), 95 (2008).

[13] X. Gu, Y. Guo, F. Zhang, A. M. Mebel, and R. I. Kaiser, Faraday Discuss. **133**, 245 (2006).

[14] X. Gu, Y. Guo, E. Kawamura, and R. I. Kaiser, J. Vac. Sci. Technol. A **24**(3), 505 (2006).

[15] X. Gu, F. Zhang, and R. I. Kaiser, J. Phys. Chem. A **112**(39), 9607 (2008).

[16] X. Tan, *Diatomic* (CyberWit, Santa Clara, 2004).

[17] F. Melen, I. Dubois, and H. Bredohl, J. Phys. B **18**(12), 2423 (1985).

[18] H. S. Liszt and W. H. Smith, J. Quant. Spectrosc. Radiat. Transf. **11**(7), 1043 (1971).

[19] M. A. A. Clyne and M. C. Heaven, Chem. Phys. **51**(3), 299 (1980).

[20] F. J. Melendez, L. Sandoval, and A. Palma, J. Mol. Struct.: THEOCHEM **580**, 91 (2002).

[21] R. N. Schwartz, Z. I. Slawsky, and K. F. Herzfeld, J. Chem. Phys. **20**(10), 1591 (1952).

[22] S. Ergun and J. T. McCartney, Proceedings of the Fifth Conference on Carbon **2**, 167 (1963).

[23] S. Hay, F. Shokoohi, S. Callister, and C. Wittig, Chem. Phys. Lett. **118**(1), 6 (1985).

[24] G. A. Bethardy, F. J. Northrup, and R. G. Macdonald, J. Chem. Phys. **105**(11), 4533 (1996).

[25] G. A. Bethardy, A. F. Wagner, G. C. Schatz, and M. A. ter Horst, J. Chem. Phys. **106**(14), 6001 (1997).

[26] F. Leonori, K. M. Hickson, S. D. Le Picard, X. Wang, R. Petrucci, P. Foggi, N. Balucani, and P. Casavecchia, Mol. Phys. **108**(7–9), 1097 (2010).